

The temperature-dependent defect density of a-Si:H calculated from thermally activated conductivity

This article has been downloaded from IOPscience. Please scroll down to see the full text article.

1992 J. Phys.: Condens. Matter 4 10433

(<http://iopscience.iop.org/0953-8984/4/50/031>)

View [the table of contents for this issue](#), or go to the [journal homepage](#) for more

Download details:

IP Address: 171.66.16.159

The article was downloaded on 12/05/2010 at 12:43

Please note that [terms and conditions apply](#).

The temperature-dependent defect density of a-Si:H calculated from thermally activated conductivity

V Kirbs, T Drüsedau† and H Fiedler

Fakultät für Naturwissenschaften, Institut für Experimentelle Physik der Technischen Universität 'Otto von Guericke' Magdeburg, PSF 4120, O-3010 Magdeburg, Federal Republic of Germany

Received 1 June 1992, in final form 30 September 1992

Abstract. The thermally activated conductivity of undoped a-Si:H films, prepared by glow discharge and magnetron sputtering, was measured by cooling samples down from 453 K to 306 K at a rate of 0.3 K min⁻¹. This resulted in systematic and reproducible deviations from straight lines in the $\ln \sigma$ versus $1/T$ plot, and from these data the Fermi level shift was determined. By means of a density of states model adapted to each sample, combining electrical, optical and ESR measurements, the temperature-dependent defect density was calculated from the charge conservation law.

The results are explained by a non-monotonic temperature-dependent defect density below the equilibrium temperature in undoped a-Si:H. The thermally induced changes increase with increasing hydrogen content of the samples. Films of identical hydrogen content show similar behaviour, independent of the preparation technique.

1. Introduction

Recently, an increasing number of papers (Smith and Wagner 1985, Smith *et al* 1986, Kakalios and Street 1986) have reported on metastable effects in doped and undoped hydrogenated amorphous silicon (a-Si:H). Furthermore, it has been demonstrated that the density of states (DOS) related to dangling bonds (DB) and doping states is in thermal equilibrium above an equilibrium temperature T_E . After high temperature annealing, two regions of different behaviour separated by the equilibrium temperature T_E have been observed. Above T_E the electrical properties are independent of previous thermal treatments. Below T_E a 'freezing in' of the DOS is found and the thermally activated conductivity $\sigma(T)$ is strongly influenced by previous thermal treatment (Street *et al* 1986).

A number of models describing the thermal equilibrium defect density in undoped a-Si:H have been presented (Smith *et al* 1986, McMahon and Tsu 1987, Xu *et al* 1988). In particular, model calculations for thermal equilibrium processes including the thermodynamics of the creation of neutral defects from weak bonds connected with the motion of bonded hydrogen show an increase of the equilibrium defect density with temperature. These results are in good agreement with experimental findings for the temperature-dependent defect density above T_E deduced from ESR measurements (Street and Winer 1989, and references therein). In contrast to this, Lee *et al*

† Present address: Division of Applied Sciences, Harvard University, Cambridge, MA 02138, USA.

(1987) observed a slow increase of the spin density after rapid quenching to room temperature. Further, the present authors reported on a non-monotonic temperature-dependent defect density for a-Si:H with a minimum at about 450 K and a maximum at about 370 K (Druesedau *et al* 1992). The data were derived from measurements of slow cooling $\sigma(T)$ as well as from quenching experiments, and afterwards conductivity measurements at room temperature and DOS spectroscopy by CPM. Hence, additional experimental and theoretical studies of the thermal equilibrium defect density below T_E seem to be necessary.

The aim of this paper is to determine the temperature-dependent defect density of undoped a-Si:H below its equilibrium temperature by means of temperature-dependent conductivity measurements at slow cooling rates and complementing measurements. The influence of the preparation method, the hydrogen content of films and the cooling rates used for conductivity experiments on thermally induced metastable changes is described. Finally, the relaxation of the dark conductivity σ at different temperatures compared with the calculated temperature behaviour of the defect density will be discussed.

2. Experimental details and results

The conductivity measurements were carried out as follows. Samples were heated up to 453 K at a rate of 3 K min⁻¹ and kept there for 10 min. Hereafter, conductivity measurements were performed during cooling from 453 K to 306 K at a rate of 0.3 K min⁻¹. The measurements were accomplished by an electrical field of $E = 1000$ V cm⁻¹ (ohmic behaviour) under vacuum conditions (pressure below 10⁻¹ Pa) and in a coplanar electrode arrangement with evaporated electrodes of 1 mm interelectrode spacing. The electrode materials were Cr, NiCr or Al for glow discharge (GD) a-Si:H and Al for sputtered (MSP) a-Si:H.

The coplanar geometry can be used to study the metastability of undoped a-Si:H because modifications of adsorbate layers during thermal treatment are too small to induce electrical changes comparable to that induced by metastabilities. This is confirmed by very similar metastable effects for the conductivity of a-Si:H using coplanar and sandwich configurations (Meaudre *et al* 1990).

The investigated GD samples were prepared under optimum conditions (device quality) in the laboratories of the Universities of Marburg, Prague and Kaiserslautern, with a typical thickness of 900 nm. Further, a set of magnetron sputtered films of typical 600 nm thickness (Druesedau *et al* (1988) at the University of Magdeburg) was investigated. These samples deposited under identical conditions, with the exception of the varying hydrogen partial pressure, are of high photosensitivity, with $\sigma_{PH}/\sigma_D = 10^5$ at maximum. The hydrogen content H/Si was determined by means of infrared spectroscopy (Shanks *et al* 1980, Druesedau *et al* 1988). The amount of hydrogen content increases monotonically with sample number (#201–#206) between 9 and 28%.

A typical result of the experiment described above is shown in figure 1. Deviations of the $\sigma(T)$ curves from the Arrhenius equation

$$\sigma(T) = \sigma_0 \exp(-E_A/kT) \quad (1)$$

are evident for both MSP and GD a-Si:H. Three repetitions of the experimental procedure within a period of six months gave good reproducibility of these curves.

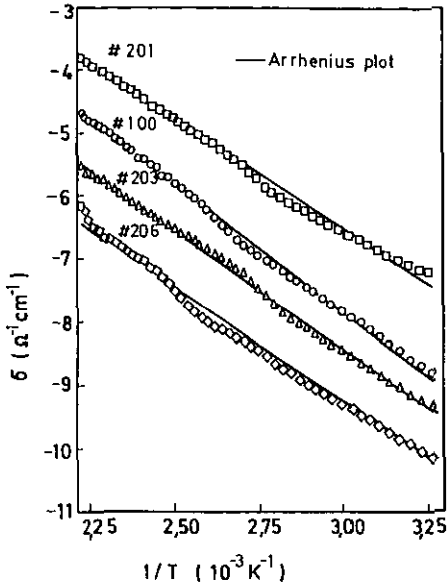


Figure 1. The temperature dependence of the DC dark conductivity σ (Arrhenius plot) measured for magnetron sputtered (samples #201, #203, #206) and glow discharged a-Si:H (sample #100).

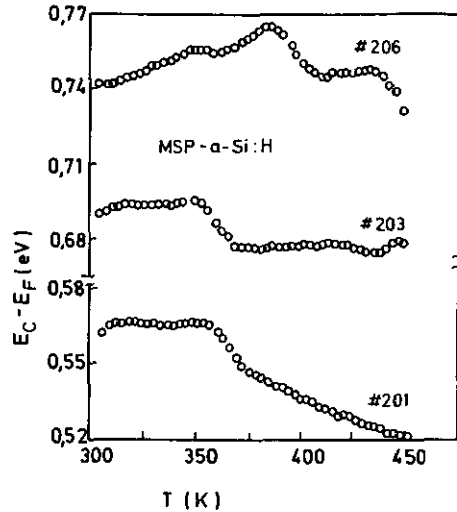


Figure 2. The energy difference ($E_C - E_F$) as a function of temperature T for magnetron sputtered films of different hydrogen contents: #201, H/Si = 9.5%; #203, 22.5%; #206, 28%.

The temperature-dependent position of the Fermi level E_F with respect to the conduction band mobility edge E_C can be calculated by the transport formula (Fritzsche 1971)

$$\sigma(T) = \sigma_M \exp\{-[E_C(T) - E_F(T)]/kT\} \quad (2)$$

which describes the thermally activated conductivity above E_C . The fundamental prefactor was taken to be $\sigma_M = 100 \Omega^{-1} \text{cm}^{-1}$ (Mott 1985, Overhof and Thomas 1989).

Figure 2 presents the $(E_C - E_F)$ data obtained for MSP a-Si:H. In contrast to the assumption of a linear shift (Jones *et al* 1977, Druessedau *et al* 1987), usually made and valid in the case of 'fast' cooling, the $(E_C - E_F)(T)$ curves are non-linear. Their shape is influenced by the hydrogen content.

Figure 3 displays $(E_C - E_F)(T)$ curves derived from figure 1 for GD films exhibiting smaller deviations from linear shape than in the case of MSP material. Additionally, measurements of the thermally activated conductivity under improved vacuum conditions ($p < 10^{-3}$ Pa) were performed for various samples. Figure 3 presents a comparison between $(E_C - E_F)(T)$ data derived for sample #100 from measurements at the two different vacuum pressures. We did not find any significant influence of the decreased pressure on the conductivity, as evident from figure 3. Probably, the main reason for this can be referred to an equilibrium contamination of the sample surface throughout, since the samples were exposed to air for a longer time after preparation and were never exposed to UHV. Hence, the influence of adsorbates at the surface of films measured at $p = 10^{-1}$ Pa can be neglected.

Figures 2 and 3 show that the strongest temperature dependence of $(E_C - E_F)$ expressed in terms of $\Gamma = d(E_C - E_F)/dT$ occurs at $370 \text{ K} < T < 390 \text{ K}$ for GD

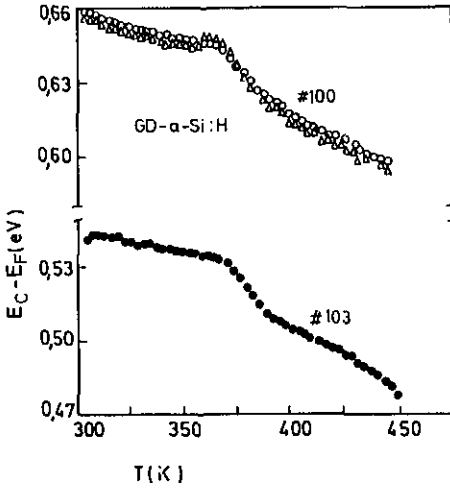


Figure 3. The energy difference ($E_C - E_F$) as a function of temperature T for two glow discharge films. The measurements for sample #100 were performed under different vacuum conditions: circles, 10^{-1} Pa; triangles, 10^{-3} Pa.

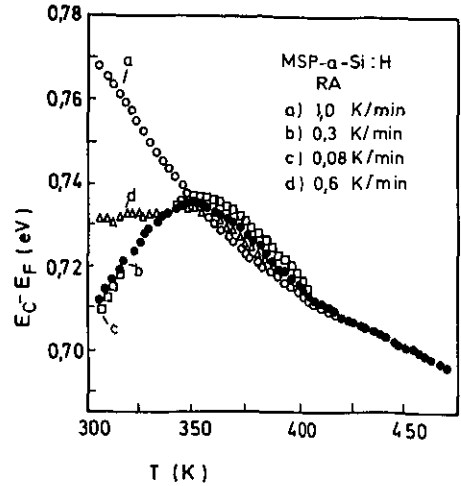


Figure 4. The influence of the cooling rate R_A on the temperature dependence of the $(E_C - E_F)(T)$ data.

($\Gamma \simeq -1.3 \text{ meV K}^{-1}$) and at $355 \text{ K} < T < 375 \text{ K}$ for MSP material with a lower hydrogen content ($\Gamma \simeq -1.2 \text{ meV K}^{-1}$).

For the investigation of the influence of cooling rates on the thermally activated conductivity, an MSP sample with a hydrogen content of 10% was measured at different cooling rates R_A in a range from 0.08 to 1 K min^{-1} . Figure 4 illustrates that a variation of R_A leads to a splitting of the $(E_C - E_F)(T)$ curves below $T = 420 \text{ K}$. Below this temperature a decrease of the cooling rate causes a strong deviation from a linear shift of $(E_C - E_F)(T)$, which is expected for fast cooling.

Further on, the GD film #103 is annealed at 453 K for 10 min, and after that follows a rapid quenching of this sample of about 600 K min^{-1} to $T = 423 \text{ K}$ and in a second cycle to $T = 373 \text{ K}$. According to this procedure, figure 5 displays the time behaviour of the conductivity after quenching. This time dependence has been normalized by plotting

$$\sigma_N(t) = (\sigma(t) - \sigma_{\text{MIN}}) / (\sigma_{\text{MAX}} - \sigma_{\text{MIN}}) \quad (3)$$

the values σ_{MAX} and σ_{MIN} being the maximum and minimum conductivities, respectively, occurring throughout a time evolution of 100 min. Note that for the same sample the relaxation process leads to an increase of the conductivity with time (at $T = 423 \text{ K}$) as well as to its decay (at $T = 373 \text{ K}$).

3. Numerical model

An explanation of the results presented above is suggested by the basic assumption that the strong shift of E_F observed due to thermal effects is a result of temperature-dependent changes of the DOS below E_F (for example, weak bond-dangling bond

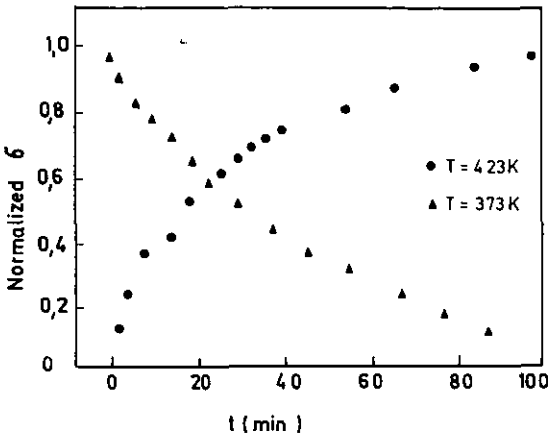


Figure 5. The relaxation of the normalized conductivity $\sigma_N(t)$ in glow discharged a-Si:H at different temperatures after quenching from 453 K (for details see text).

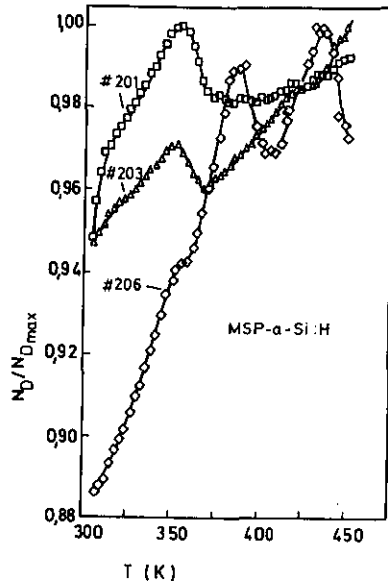


Figure 6. The calculated normalized dangling bond density N_D versus temperature T for the three magnetron sputtered a-Si:H samples of figure 1.

conversion (Stutzmann 1987)). The basis of the calculations is a DOS model composed of exponential band tails and gaussian shaped DB densities:

$$\begin{aligned}
 N_{VB}(E) &= N_V = \text{constant} & (E < E_V) \\
 N_{VB}(E) &= N_V \exp[(E_V - E)/E_{V0}] & (E > E_V) \\
 N_{CB}(E) &= N_C = \text{constant} & (E > E_C) \\
 N_{CB}(E) &= N_C \exp[(E - E_C)/E_{C0}] & (E < E_C) \\
 N_{DB}(E, T) &= N_D(T) / \exp[(E_D - E)/E_{D0}]^2
 \end{aligned} \tag{4}$$

where $N_{VB}(E > E_V)$, $N_{CB}(E < E_C)$ and $N_{DB}(E, T)$ are, respectively, the contributions of the valence and conduction band tail and the DB to the DOS in the mobility gap of undoped a-Si:H. The DOS $N_{VB}(E < E_V)$ and $N_{CB}(E > E_C)$ in the valence band and conduction band is given by N_V and N_C , respectively. The modelling of thermal effects which are known to arise from variations of the DB density (Xu *et al* 1989) was realized by the assumption of a temperature-dependent peak height $N_D(T)$ of the gaussian shaped dangling bond DOS, i.e. net 'production' or 'reduction' of electronic states. Note that this idea cannot explain the behaviour of 'real intrinsic' a-Si:H, where E_F is pinned independent of a changed defect density, because of the balance between created and annihilated electronic states below the Fermi level.

From the literature, standard parameters for the model DOS were chosen to be: DOS at the mobility edges, $N_C = N_V = 10^{21} \text{ eV}^{-1} \text{ cm}^{-3}$; correlation energy, $U = 0.3 \text{ eV}$; and the width of DB distribution, $E_{D0} = 140 \text{ meV}$ (Le Comber and Spear 1986).

Furthermore, from measurements of fundamental and subgap optical absorption at room temperature for each sample one gets the optical Tauc gap and the characteristic energy of the valence band tail E_{V0} , respectively. The mobility gap $E_G = E_C - E_V$ can be replaced approximately by the optical Tauc gap (Druesedau 1991). Here, we suppose a temperature-independent value E_{V0} according to experimental results by Aljishi *et al* (1990). Also, from CPM measurements in the tail state absorption regime ($h\nu > 1.4$ eV) it has been deduced that thermal changes of the DOS are not related to variations of E_{V0} (Xu *et al* 1989). The characteristic energy of the conduction band tail was taken to be $E_{C0} = 0.55 E_{V0}$, according to the literature (Fritzsche 1985).

A linear temperature dependence of the optical gap (after Tauc *et al* 1966) above room temperature was found in agreement with other authors (e.g. Ley 1984). The linear fit to temperature-dependent $(E_C - E_F)$ data deduced from $\sigma(T)$ measurements at a faster cooling rate for a variety of samples (see curve a in figure 4) for example yields a shift coefficient $\Gamma \simeq 5k$ where the position of the Fermi level below T_E is assumed to be fixed due to small changes of the DOS and a negligible statistical shift (Overhof and Thomas 1989, Druesedau *et al* 1987). For this case the temperature dependence of $(E_C - E_F)$ is a result of the E_C shift only. Hence shift coefficients $\Gamma_C = dE_C/dT = 5k$ and $\Gamma_V = dE_V/dT = 0$ were used in agreement with Overhof and Thomas (1989).

The energetic position of the neutral DB density peak was determined by

$$E_D = E_G^+ - (E_C - E_F)^+ - U/2 + \delta E \quad (5)$$

where E_G^+ is the mobility gap at zero temperature derived from $E_G(T)$ measurements in the range $80 \text{ K} \leq T \leq 296 \text{ K}$ and an Einstein oscillator fit (Cody 1984). The parameter $(E_C - E_F)^+$ is the 'median' activation energy of thermally activated conductivity. Consequently, the energy value δE is referred to as 'unintentional doping' by such impurity atoms as N and O and an uncertainty of $(E_C - E_F)$ data at zero temperature.

The value of $N_D(T)$ at room temperature was estimated from the dangling bond density (n_S) measured by ESR, PDS and CPM:

$$\bar{n}_S = \int_{E_V}^{E_C} N_{DB}(E, T) f_1(E, T) dE$$

$$f_1 = \frac{2 \exp[-\beta(E - E_F)]}{1 + 2 \exp[-\beta(E - E_F)] + \exp[-\beta(2E - 2E_F + U)]} \quad (6)$$

Using the model parameters derived, the temperature-dependent peak height of the defect density $N_D(T)$ can be calculated by means of the charge conservation law:

$$\int_{-\infty}^{+\infty} [N_{VB}(E) + N_{CB}(E)] f(E, T) dE + \int_{E_V}^{E_C} N_{DB}(E, T) f_2(E, T) dE = \text{constant} \quad (7)$$

where f is the Fermi-Dirac distribution function and f_2 is the distribution for two-electron states:

$$f_2 = \frac{2 \exp[-\beta(E - E_F)] + 2 \exp[-\beta(2E - 2E_F + U)]}{1 + 2 \exp[-\beta(E - E_F)] + \exp[-\beta(2E - 2E_F + U)]} \quad (8)$$

with $\beta = 1/kT$ (Bonch-Bruевич *et al* 1984).

4. Results of model calculation

To examine the influence of the assumptions made in the model, the dependence of $N_D(T)$ curves on different parameters Γ_C ($2.5k$, $5k$), E_{D0} (120 meV– 160 meV), E_{C0} ($\pm 10\%$) and δE ($+50$ to -50 meV) was investigated. The results indicate that variations of these data may influence the absolute values of $N_D(T)$, but do not change the qualitative behaviour. Hence, the curves in figures 6 and 8 can be extended or contracted by a factor of two, which also induces a change of the ratio $N_{D\text{MAX}}/N_{D\text{MIN}}$ (see figure 7).

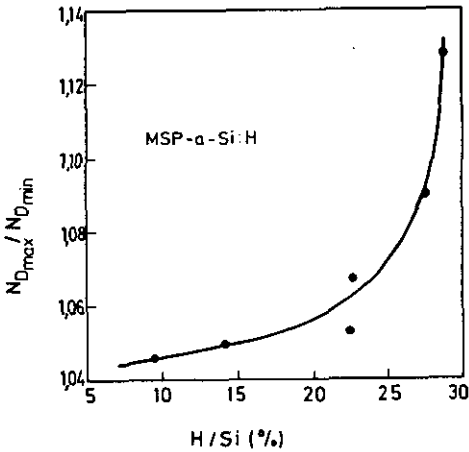


Figure 7. The ratio of maximum to minimum $N_D(T)$ versus hydrogen content $c_H = H/Si$ for a set of magnetron sputtered a-Si:H samples.

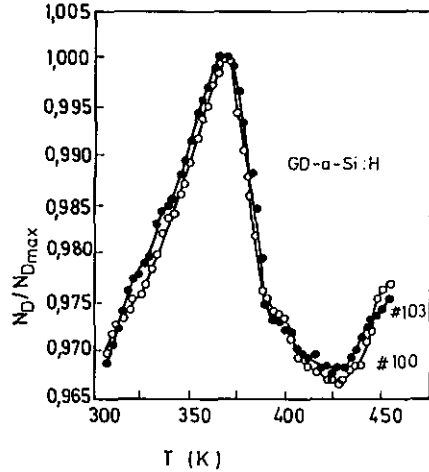


Figure 8. The calculated normalized dangling bond density N_D as a function of temperature T for two glow discharge films.

The calculated peak height $N_D(T)$ of the DB density, which in the following is used synonymously as the defect density, normalized to its maximum value $N_{D\text{MAX}}$, is represented for MSP films in figure 6. The curves exhibit an increase of N_D with temperature up to 355 K. In contrast to the N_D decay at 355 K $< T < 375$ K (#201, #203) samples with higher hydrogen content (#206) show increasing values. Above 375 K for samples #201 and #203 one gets an increasing $N_D(T)$ curve, but for sample #201 the maximum at 355 K is not reached again. However, a higher level of hydrogen incorporation (#206) results in a stronger structured $N_D(T)$ curve of MSP materials.

Figure 7 displays the ratio of maximum to minimum $N_D(T)$ derived for all sputtered samples. The values $N_{D\text{MAX}}/N_{D\text{MIN}}$ are strongly dependent on the hydrogen content of the films, especially above $c_H = H/Si = 20\%$.

Further, $N_D(T)$ values calculated from two selected GD films are plotted in figure 8. After increasing $N_D(T)$ with temperature, up to a maximum between 370 K and 375 K, a remarkable drop of N_D up to 425 K follows. At higher temperatures the $N_D(T)$ curves increase again. These GD samples have a typical value of $c_H \approx 10\%$.

In figure 9 it is shown that the decrease of R_A results in growing changes of the temperature-dependent defect density for a given temperature range. According to the experimental procedure chosen here, below $T = 420$ K the $N_D(T)$ behaviour

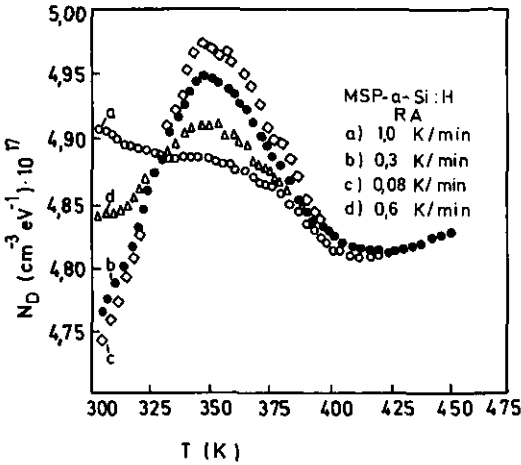


Figure 9. The influence of the cooling rate R_A on thermally induced changes of the defect density $N_D(T)$ for a magnetron sputtered film.

is sensitive to the rate at which the samples were cooled. Decreasing cooling rates are related to an upward shift of the equilibrium temperature T_E by about 20 K. From this figure the good qualitative agreement of $N_D(T)$ curves resulting from measurements at $R_A \leq 0.6 \text{ K min}^{-1}$ is evident. It should be noted in this context that, for example, the N_D maxima obtained at about 355 K differ from each other only by about 1%.

5. Discussion

The bulk nature of the effect observed is evident from recent work (Stutzmann *et al* 1985, Kakalios and Street 1988, Xu *et al* 1988, Meaudre *et al* 1990). Further, from measurements for a set of a-Si:H samples of different sample thicknesses d_s it was demonstrated that, at least above $d_s = 500 \text{ nm}$, the observed thermally induced conductivity changes are related to the bulk of the films (Druessedau *et al* 1992). Additionally, results identical to those reported above were obtained from thick (up to $4 \mu\text{m}$) GD a-Si:H films with metallic or NiCr/n⁺-a-Si:H injecting coplanar contacts (Druessedau *et al* 1991). So one is able to exclude the role of film surface as well as of the metal contacts on the observed effect in conductivity.

Taking into consideration the E_C shift, the differential temperature coefficient Γ_F becomes too large to be caused by the temperature dependence of the distribution function (statistical Fermi level shift) which is computed in several publications (Overhof and Beyer 1981, Yoon *et al* 1986, Druessedau *et al* 1987). Hence the existence of an additional shift component due to alterations of the DOS with temperature must be assumed (Smith *et al* 1986, Redfield 1988).

Obviously, a characteristic thermal spectrum of defect states exists in all a-Si:H films. This is confirmed by an additional quenching experiment we applied to one selected GD sample of $1 \mu\text{m}$ thickness as follows: annealing for 2 h at $T_A = 503, 473, \dots, 323 \text{ K}$ under vacuum followed by rapid quenching at a rate of about 40 K s^{-1} to room temperature. Hereafter, measurements of the dark conductivity, photoconductivity, and the defect density by means of the CPM technique detecting changes of the excess absorption were accomplished. A more detailed description of several methods for the analysis of the temperature-dependent defect

density has been given recently (Druessedau *et al* 1992). However, the comparison between our model calculations deduced from thermally activated conductivity during slow cooling with independent experimental findings of subgap absorption, as well as conductivity measurements after thermal quenching, leads to the conclusion that a non-monotonic temperature dependence of the defect density below T_E is a general feature of intrinsic a-Si:H. Thus, the previously existing model for the description of thermal equilibrium (Street and Winer 1989) might be invalid for the case of temperatures below T_E .

The experimental procedure applied above enables at lower temperatures, as a consequence of increasing relaxation time only, an approximated saturation value of the dark conductivity. In particular, as indicated in figure 9, $\sigma(T)$ measurements between 453 K and 306 K in the thermal equilibrium state of defect density can be expected only at cooling rates which are much smaller than 0.08 K min^{-1} . On the other hand, very similar $N_D(T)$ curves result from measurements at 0.3 K min^{-1} and 0.08 K min^{-1} , respectively, and therefore we conclude that significant information about the temperature-dependent defect density will certainly be obtained at a cooling rate of 0.3 K min^{-1} .

The derived $N_D(T)$ curves of GD and MSP samples of low hydrogen content (#201) exhibit a similar shape to those found for the temperature dependence of the steady-state metastable defect density (Redfield 1988).

Samples containing an identical amount of hydrogen $\sim 10\%$ (#201, #103, #100) exhibit $N_D(T)$ curves of similar shape, independent of their preparation method (please note the different scales of figures 6 and 8). However, the positions of minima and maxima of $N_D(T)$ are located at different temperatures. So, N_D maxima and minima determined for GD material appear at temperatures exceeding that obtained from MSP material by about 20 K and 35 K, respectively.

Likewise, thermal equilibrium processes have been studied recently in undoped RF glow discharge and DC sputtered films by analysing the conductivity after annealing and subsequent cooling at different rates (Meaudre *et al* 1988a, b). Here, the authors found different equilibrium temperatures for their GD ($T_E = 453 \text{ K}$) and MSP ($T_E = 418 \text{ K}$) films.

Exploitation of our results about a thermally induced metastable defect density enables a clearer understanding of experimental findings elsewhere (Meaudre *et al* 1988a, b). In particular, the existence of different values for T_E can be explained as follows.

First, the N_D maximum obtained for samples with a lower hydrogen content occurs below T_E . It has been shown that changes of the defect density with temperature in GD material above 400 K are stronger than the N_D variations in MSP films depicted in figures 6 and 8. Obviously, such stronger thermal changes of the defect density in GD samples seem to explain that at the higher cooling rate of 600 K min^{-1} used experimentally (Meaudre *et al* 1988a, b), the defect density cannot follow its saturation value any longer during cooling, and, therefore, the freezing in of the defect density already starts at about $T_E = 453 \text{ K}$. In contrast to this, because of the smaller temperature gradient determined for MSP material, the defect density is able to persist at equilibrium, even at lower temperatures of up to about 418 K, according to the cooling rate used. Certainly, at lower cooling rates (near 1 K min^{-1}) the DOS will be able to relax into its equilibrium value for longer and thus, different $\sigma(T)$ curves occur below T_E .

Also, the different temperatures of the $N_D(T)$ extrema established in GD and

MSP films emphasize the occurrence of different equilibrium temperatures in these materials.

Further, Meaudre *et al* (1988a, b) have given a review of isothermal relaxation processes. It was found that below T_E the non-equilibrium dark conductivity referred to as thermal quenching is reduced in GD films and increased in MSP films in comparison with its equilibrium value.

The results for MSP and GD films calculated in this work will be used to interpret the isothermal relaxation behaviour reported by Meaudre *et al* (1988a, b) as follows.

We suppose that at a fixed temperature, an increase of the DOS around E_F will always shift the Fermi level to lower energies and, vice versa, a decreasing DOS causes the Fermi level to move to higher energies. Hence, for the understanding of different experimental results for isothermal treatment with respect to the preparation method, we propose the following.

The temperatures applied for investigations of relaxation behaviour in MSP a-Si:H are mainly in the range of the computed N_D maximum (see figure 6, #201). Obviously, during quenching from 473 K to room temperature at 600 K min^{-1} the DB density will be frozen in at its $N_D(T_E)$ value and following isothermal treatment effects a relaxation from a low defect density into a higher one at lower temperatures. The increase of DOS with time causes an upward shift of E_F in correspondence with the decay of 'excess' conductivity observed.

Contrarily, relaxation temperatures applied to GD films are in the range of the N_D minimum (see sample #100). The 'freeze in' after rapid quenching (600 K min^{-1}) certainly occurs at temperatures above the relaxation temperature since longer relaxation times in GD material could be proved (Meaudre *et al* 1988a, b). Thus, during an immediate isothermal process, a decrease of defect density is possible connected with a 'reduced' conductivity increasing to its steady state value.

Also, the experimental findings about the relaxation process shown in figure 5 can be explained in the same manner by the $N_D(T)$ curve for this film (figure 8, #103) and are clear experimental evidence for a non-monotonic temperature-dependent defect density and a different time behaviour of the conductivity after rapid thermal quenching observed elsewhere (Meaudre *et al* 1988a, b) also. Consequently, the experimental observation of a decrease or increase in conductivity for MSP a-Si:H during isothermal treatment carried out at different temperatures between 453 K and 333 K (see figure 1 in Kirbs *et al* 1990) seems to be plausible. In the literature (Stutzmann *et al* 1985, Stuke 1987, Street *et al* 1987) it is supposed that hydrogen diffusion is the main underlying mechanism determining defect equilibrium. Ohsawa *et al* (1985) and Pinarbasi *et al* (1990) show that GD and MSP films with a lower hydrogen content are more stable against light irradiation. According to these authors: (i) similar qualitative alterations of the defect density could be observed in MSP as well as GD samples of identical hydrogen content and (ii) a higher hydrogen content leads to stronger changes of the defect density (compare figure 7). Quite commonly, these results are a further argument that in a-Si:H independent of the generation process a close correlation exists between the excited metastable defects and the concentration of incorporated hydrogen.

Noting that films with lower hydrogen content have the highest DOS, it is clear that the initial DOS is not a reliable quantity of thermal metastability, which is in good agreement with observations of light induced effects (Pinarbasi *et al* 1990, Park *et al* 1990).

6. Summary and conclusions

Investigations of thermal activated dark conductivity in undoped a-Si:H at a slow cooling rate show strong deviations of $\sigma(T)$ curves from the Arrhenius equation, caused by thermal changes of the defect density.

The resulting shift coefficients dE_F/dT whose absolute values partially exceed 1.3 meV K^{-1} are assumed to be the result of temperature-dependent gap state changes superposing the 'statistical shift'.

A method for the determination of the temperature-dependent defect density experimentally founded on measurements of the thermally activated conductivity is presented for undoped a-Si:H. The numerical calculations were performed on the basis of a DOS model adapted to each sample under consideration of the charge conservation law.

In particular, it is argued that the defect density of intrinsic a-Si:H is distinguished by the non-monotonic behaviour with temperature. The main feature of the defect density in GD and MSP material of device quality containing about 10% hydrogen is the existence of a minimum below the equilibrium temperature.

Generally, the thermal behaviour of the DOS in GD material is qualitatively similar to that observed for MSP films with identical hydrogen content. The higher content of hydrogen in sputtered a-Si:H causes stronger changes of the defect density with temperature. This is attributed to an enhanced hydrogen diffusion.

Summarizing the results for MSP samples indicates that the influence of the hydrogen content on the thermal stability of electronic properties seems to be stronger than the influence of the absolute DB concentration.

The interpretation of the existence of different equilibrium temperatures and isothermal relaxation behaviour in MSP and GD a-Si:H is related to slight differences in the temperature dependence of the defect density.

Acknowledgments

We wish to acknowledge the following colleagues for valuable discussions and for providing us with samples: Professor P Thomas and Dr H Mell (University of Marburg), Dr J Kocka (University of Prague), Dr M Stutzmann (Max-Planck-Institut, Stuttgart), Dr M Hoheisel (Siemens AG, Munich) and Dr B Schroeder, Mrs U Schmidt and Mr B Schehr (University of Kaiserslautern).

References

- Aljishi S, Cohen J D, Jin S and Ley L 1990 *Phys. Rev. Lett.* **64** 2811
- Bonch-Bruевич V L, Enderlein R, Esser B, Keiper R, Mironov A G and Zvyagin B 1984 *Electronic Theory of Disordered Semiconductors* (Berlin: VEB Deutscher Verlag der Wissenschaften) (in German)
- Cody G D 1984 *Hydrogenated Amorphous Silicon-Optical Properties (Semiconductors and Semimetals 21B)* ed R K Willardson and A C Beer (New York: Academic) p 46
- Druesedau T 1991 *Phys. Status Solidi* b **168** K65
- Druesedau T, Eckler M and Bindemann R 1988 *Phys. Status Solidi* a **108** 285
- Druesedau T, Kirbs V and Fiedler H 1991 *Mater. Res. Soc. Symp. Proc.* **219** 123
- 1992 *Solid State Commun.* **82** 359
- Druesedau T, Wegener D and Bindemann R 1987 *Phys. Status Solidi* b **140** K27
- Fritzsche H 1971 *J. Non-Cryst. Solids* **6** 49

- Fritzsche H 1985 *J. Non-Cryst. Solids* **77-8** 273
- Jones D I, Le Comber P G, Spear W E 1977 *Phil. Mag.* **36** 541
- Kakalios J and Street R A 1986 *Phys. Rev. B* **34** 6014
- 1988 *Thermal Equilibrium Effects in Doped Hydrogenated Amorphous Silicon, Amorphous Silicon and Related Materials* ed H Fritzsche pp 165-205
- Kirbs V, Druessedau T and Fiedler H 1990 *J. Phys.: Condens. Matter* **2** 7473
- Le Comber P G and Spear W E 1986 *Phil. Mag. Lett.* **53** 1
- Lee C, Ohlsen D and Taylor P C 1987 *Phys. Rev. B* **36** 2965
- Ley L 1984 *Topics Appl. Phys.* **56** 61
- McMahon B and Tsu E 1987 *Appl. Phys. Lett.* **51** 412
- Meaudre R, Jensen P and Meaudre M 1988a *Phys. Rev. B* **38** 12 449
- Meaudre R, Meaudre M, Jensen P and Guiraud G 1988b *Phil. Mag. Lett.* **57** 6
- Meaudre M, Meaudre R and Jensen P 1990 *J. Non-Cryst. Solids* **122** 312
- Mott N F 1985 *Phil. Mag.* **B 51** 19
- Ohsawa M, Hama T, Akasak T, Ichimara T, Sakai H, Ishida S and Yishiyuki U 1985 *Japan. J. Appl. Phys.* **24** 838
- Overhof H and Beyer W 1981 *Phys. Status Solidi* **b 107** 207
- Overhof H and Thomas P 1989 *Electronic Transport in Hydrogenated Amorphous Semiconductors (Springer Tracts in Modern Physics 114)* (Berlin: Springer) p 169
- Park H R, Liu J Z, Roca i Cabaroccas P, Maruyama A, Isomura M, Abelson J R and Finger F 1990 *Appl. Phys. Lett.* **57** 14
- Pinarbasi M, Abelson J R and Kushner M J 1990 *Appl. Phys. Lett.* **56** 17
- Redfield D 1988 *Appl. Phys. Lett.* **52** 6
- Shanks H, Fang C J, Ley L, Cardona M, Demond F J and Kalbitzer S 1980 *Phys. Status Solidi* **b 100** 43
- Smith Z E, Aijishi S, Slobodin D, Chu V, Wagner S, Lenahan P M, Arya R R and Benett M S 1986 *Phys. Rev. Lett.* **57** 2450
- Smith Z E and Wagner S 1985 *Phys. Rev. B* **32** 5510
- Street R A, Kakalios J and Hayes T M 1986 *Phys. Rev. B* **34** 3030
- Street R A, Kakalios J, Tsai C C and Hayes T M 1987 *Phys. Rev. B* **35** 1316
- Street R A and Winer K 1989 *Phys. Rev. B* **40** 6236
- Stuke J 1987 *J. Non-Cryst. Solids* **97-8** 1
- Stutzmann M 1987 *Phil. Mag.* **B 56** 63
- 1989 *Phil. Mag.* **B 60** 4
- Stutzmann M, Jackson W B and Tsai C C 1985 *Phys. Rev. B* **32** 23
- Tauc J, Grigovovici R and Vancu A 1966 *Phys. Status Solidi* **15** 627
- Xu X, Morimoto A, Kumeda M and Shimizu T 1988 *Appl. Phys. Lett.* **52** 622
- 1989 *Mater. Res. Soc. Symp. Proc.* **149** 143
- Yoon B G, Lee C and Jang J 1986 *J. Appl. Phys.* **60** 673